Hindawi
Geofluids
Volume 2018, Article ID 7418140, 9 pages
https://doi.org/10.1155/2018/7418140

Research Article

Non-Fickian Solute Transport in a Single Fracture of Marble Parallel Plate

Xiaosan Yan, Jiazhong Qian, Lei Ma, Mu Wang, and Aofeng Hu

School of Resources and Environmental Engineering, Hefei University of Technology, Hefei 230009, China

Correspondence should be addressed to Lei Ma; lei8505@hfut.edu.cn

Received 27 September 2017; Revised 30 March 2018; Accepted 23 April 2018; Published 13 June 2018

Academic Editor: Stefano Lo Russo

Accurate prediction of solute transport processes in a fracture aquifer is an important task not only for proper management of the groundwater but also for pollution control. A key issue of this task is how to accurately obtain the experimental data and to analyze the solute transport in fracture in subsurface hydrology, which would greatly help us to understand the releasing mechanism and transport of the solute in a fracture. In this study, a fracture experiment is conducted in a laboratory based on previous studies. The fracture used with a length of 60 cm and a width of 10 cm is sealed with glass glue to avoid leakage of tracer due to uneven fracture walls. The sodium chloride (NaCl) solute is injected from the left of the fracture. And an electrical conductivity monitoring system is installed on the right of the fracture. Then breakthrough curves (BTCs) of solute transport are fitted using the classical advection-dispersion equation (ADE) and the truncation power-law function (TPL) model in the package of the continuous time random walk (CTRW). The results show that the flow satisfies non-Darcian law in the experimental conditions, which can be better fitted using the Forchheimer equation and Izbash equation. The solute transport presents non-Fickian phenomena and shows a long tailing. The fitting results of the TPL model are far better than ADE in fitting the long tailing at three different flow velocities. Furthermore, electrical conductivity monitoring method not only is effective but also has an advantage of no disturbance to water and concentration fields in a fracture.

1. Introduction

Remediation of the polluted fractured aquifer is not easy due to many factors, such as the discrepancy of flow velocity between the facture and surrounding porous media and complex flow regimes in a fracture. Unfortunately, with the rapid economy development and an increase in population in recent decades, environmental pollution becomes more serious in both the surface water and groundwater [1]. Thus, accurate prediction of the solute transport in the surface and subsurface is very important for both pollution control and aquifer remediation [2]. However, the measurement and quantitative analysis of flow and solute transport in a fracture aquifer remains one of the most challenging problems in subsurface hydrology, which will be investigated in this study.

Recently, electrical property quantification has been widely used to better understand the contaminant transport in the aquifer. Kemna et al. and Jackson et al. [3, 4] have taken into account electrical resistance measurement to investigate different geotechnical parameters of the subsurface characteristics. Similarly, such a method will be employed to determine the concentration of the solute in the fracture in this study.

Tracer tests have been commonly used for benchmark experiments for investigating solute transport in facture media. The electrical conductivity monitoring system is applied to determine the concentration of the tracer. This system is helpful for the measurement and quantitative analysis of the solute transport behavior owing to accuracy and no disturbance to water and concentration fields in the fracture. This is the main contribution of this study. By reviewing the previous studies on water flow and solute transport in fracture media [1, 5–8], one may find that the measuring tracer techniques mainly included the sampling method, the digital image processing method, the concentration sensor method, the electrical resistance method (measured by digital multimeter), and the electrical conductivity monitoring method. However, the sampling method might disturb

the flow and concentration fields [5]. The digital image processing method is difficult to operate and control, and it may need a high-resolution camera and a good analytical technique [9]. The concentration sensor method can only measure the concentration of the point, where the sensors are embedded. Furthermore, a limited number of sensors can be embedded [10]. Huang et al. [1] used the electrical resistance method to determine concentration of the tracer transport in low permeability fractured rocks. A good effect was obtained; however, it may take a long time. Therefore, there is a great need for accurate measurement of water and solute transport in such a fracture. In this study, the electrical conductivity monitoring system is developed to determine the concentration of solute in the fracture aquifer. The main advantages of the electrical conductivity monitoring method over the other solute measurement methods like sampling, digital image processing, or electrical resistance include the following: (a) there is no disturbance to water and concentration fields, (b) large sets of data to assess variation of concentration fields are easily taken, (c) continuous and automatic measurement is gotten in a nondestructive real-time way, and (d) its application to fractures can help us better understand the mechanisms of flow and solute transport and find more realistic solutions to water resource problems.

For many decades, Darcy's law has been widely used to describe the flow in the subsurface. However, many recent studies demonstrated that Darcy's law only worked well for the flow in porous media with small flow velocity. Qian et al. [11–13] presented some evidence of non-Darcian flow happening in a single fracture. Wen et al. [14] also pointed out that non-Darcian flow could occur in the region near the well which fully penetrates a confined single vertical fracture. Wang et al. [15] established a two-region model considering time-dependent R_{CD}, where the non-Darcian flow was described by the Forchheimer equation. Javadi et al. [16] proposed a new geometrical model for nonlinear fluid flow through rough fractures. Cherubini et al. [17] studied non-Darcian relationship between flow rate and hydraulic loss and also found that it was best described by Forchheimer's law. Similar to non-Darcian flow, the solute transport may not follow Fick's law, such as scale-dependent spreading, early arrivals, and long tails, which are often named non-Fickian or anomalous transport. Recently, Qian et al. [13], Bauget and Fourar [18], Hadermann and Heer [19], McKay et al. [20], Kosakowski et al. [21], and Cherubini et al. [17] found non-Fickian phenomena in the solute transport and employed the advection-dispersion equation (ADE) and the continuous time random walk (CTRW) to interpret it.

The ADE model has been widely applied to describe the tracer transport in fractures. However, many studies demonstrated the significant deviations between observed and computed breakthrough curves (BTCs) in single fracture reports [18, 22–24]. Specifically, the ADE cannot capture the behaviors of the early breakthrough times and long-time tailing in BTCs, which was called the non-Fickian behavior. Up to date, there are several approaches to solve such a problem, including the equivalent-stratified medium approach proposed by Fourar [25] and subsequently applied to solute transport in a single rough-walled rock fracture [18], the MIM model which was utilized by Qian [13] to describe solute transport in a filled single fracture, and continuous time random walk (CTRW) approach [26]. Physics or geochemical mechanisms of CTRW involved in the transport process, as well as the structure of fracture media or nature of the flow regime, determine the relevant transition-time distribution and control the interpretation of its parameters. The CTRW has been successfully applied for describing the non-Fickian transport in heterogeneous porous media [27–30] and single fractures [18, 24, 31].

The main objectives of this study are to present a series of carefully designed flow and tracer transport test results of a single fracture of marble parallel plate. The following works are carried out. First, an electrical conductivity monitoring method is developed to obtain a precise concentration distribution without any disturbance to the water and concentration fields in the fracture. Second, an experimental flow and tracer transport test is performed under non-Darcian flow conditions. Subsequently, two different models including ADE and CTRW are used to simulate the experimental results, and the transport behavior in the fracture is analyzed.

2. Materials and Methods

2.1. Experimental Preparation. An experimental flow and tracer transport test is carried out in a single fracture. The marbles were taken from the nearby mountains. Then they were cut into two marble parallel plates, which were 60 cm in length, 15 cm in width, and 3 cm in height. The marble parallel plates were used for the framework of the experimental model.

Sodium chloride (NaCl) was used as the tracer. NaCl is a good tracer with some advantages. It easily dissolves in water. It also rarely reacts with the components of the rock and other materials. For these tests, the concentration of the NaCl tracer is 10 g/L.

2.2. Experimental Setup. The experimental setup consists of three components—a flow system, a single fracture of marble parallel plates, and the electrical conductivity monitoring system. The flow system is two Plexiglas flumes for discharge and recharge. The electrical conductivity monitoring system is made up of DJS-1W electrodes, data logger system, and data transmission system. Figure 1 is a schematic diagram of the experiment setup, which is modified from that of Yan et al. [32]. The fracture was constructed between two marble parallel plates. The spacing between these two plates was controlled through placement of Plexiglas strips with a height of 2.0 mm along the side edges within the fracture. Glass glue was used to waterproof the side seams of the flow pony cell. Any small gaps between the marble parallel plates were also filled with glass glue to avoid leakage of the tracer due to the uneven fractured walls. Flow through the fracture was controlled through injection of flow at a constant rate to a reservoir connected to the upstream face of the fracture and through maintenance of a constant hydraulic head at the reservoir connected to the downstream face of the fracture.

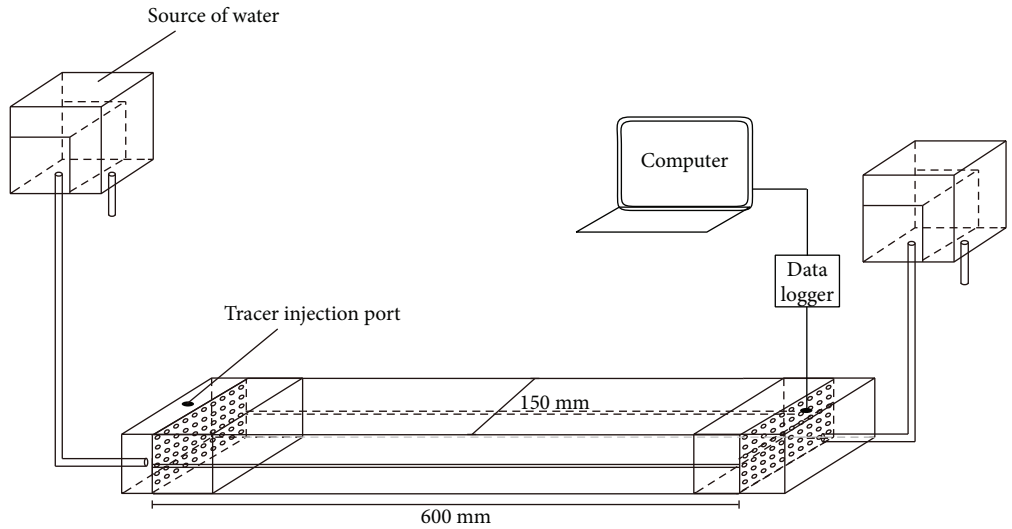

Figure 1: Schematic diagram of fracture in marble parallel plates.

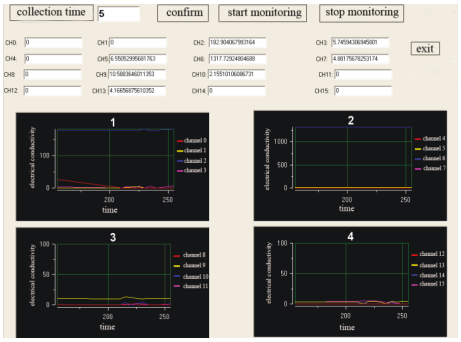

Figure 2: Data collection interface.

The Plexiglas flume of the left side is connected to the inlet of the fracture by a rubber tube. After injection of the chloride, the flow was initiated. The transport of the chloride is monitored by the electrical conductivity monitoring system. DJS-1W electrodes that are placed in a fracture medium are used to measure electrical conductivity. The measured values are sent to the data logger by digital signal shape. The data logger system carries on the processing, compiling, and outputting of digital signals. The data of conductivity is connected to a PC by a data transmission system.

2.3. Experimental Methods

2.3.1. The Measurement of Hydraulic Head Difference. The Plexiglas flumes are connected with marble parallel plates through a latex tube. After the flow is stable, the water level can be measured and hydraulic head difference can be calculated. The volume of water is collected by measuring a cylinder at the outlet of fracture.

2.3.2. The Measurement of the Tracer Concentration. During the experiments, the temperature in the laboratory was around 20°C. The concentration of the tracer was directly proportional to the electrical conductivity of the solute. The standard concentration of NaCl solution was prepared in the laboratory, then the corresponding electrical conductivities are measured using the DJS-1W electrode. The relationship of the concentration and the electrical conductivity of the tracer can be expressed as

$$\mathrm{Ec} = 42.592C + 4.1944, \tag{1}$$

where Ec is the electrical conductivity (ms/cm) and C is the concentration (g/L) of the NaCl solute. The correlation coefficient is equal to 0.9997. According to the measured electrical conductivity of the tracer, the solute concentration can be calculated by (1).

2.3.3. The Calculation of Reynolds Number. The value of Re is calculated by [11]

$$\mathrm{Re} = \frac{ve}{2\mu}, \tag{2}$$

where v is the average flow velocity in the fracture (m/s), e is the average aperture (mm), and μ is the kinematic viscosity (m^2/s). The value of μ at 20°C is $1.005 \times 10^{-6}\ \mathrm{m}^2/\mathrm{s}$.

2.3.4. Data Collection and Output System. The data collection and output system are made up of DJS-1W electrode, data logger, 24 VDC power supply, data transmission, computer, and Delphi software. Figure 2 is the data collection interface. The DJS-1W electrode can transform electrical conductivity into current signal; the data logger can collect the current signal, then the conductivity data is connected to the PC by the data transmission system.

3. Theoretical Background

3.1. Model of Flow in a Single Fracture. Darcy's law for flow in a single fracture is

$$J = \frac{v}{K}, \tag{3}$$

Table 1: Values of lost head, J, discharge (Q), v, Re, and relevant hydrodynamic parameters.

Δh (cm)	J	Q (mL/s)	v (10^{-2} m/s)	Re	Jv (10^{-2} m/s)	Ji (10^{-4} m/s)	Jv/J	Ji/J
3.0	0.050	3.409	1.136	11.303	3.999	114.965	0.800	0.230
5.0	0.083	4.974	1.658	16.498	5.837	244.894	0.703	0.295
7.0	0.117	6.440	2.147	21.363	7.558	410.652	0.646	0.351
9.0	0.150	7.670	2.557	25.443	9.002	582.467	0.600	0.388
11.0	0.183	8.920	2.973	29.582	10.466	787.407	0.572	0.430
13.0	0.217	10.050	3.350	33.333	11.793	999.768	0.543	0.460
15.0	0.250	11.050	3.683	36.647	12.966	1208.406	0.519	0.483
17.0	0.283	11.980	3.993	39.731	14.057	1420.392	0.497	0.501

where J is the hydraulic gradient, K is the hydraulic conductivity (m/s), and v is the flow velocity (m/s). A commonly used non-Darcian flow equation is the Forchheimer law:

$$J = -\left(av + bv^2\right), \tag{4}$$

where a and b are two constant coefficients.

The linear ($Jv = av$) and the quadratic terms ($Ji = bv^2$) in (4) is another method for describing the characteristic of the Forchheimer flow. These two terms are generally considered as the head loss caused by the viscosity and the inertial forces. So, (4) becomes

$$J = -(Jv + Ji). \tag{5}$$

When $Ji \gg Jv$, the inertial flow is dominating; when $Jv \gg Ji$, the viscous flow is dominating. Comparing with the value of Jv/J and Ji/J, the flow condition can be analyzed.

Another commonly used non-Darcian flow equation is the Izbash equation:

$$J = \lambda v^n, \tag{6}$$

where λ and n are two constant coefficients and $1 \le n \le 2$.

3.2. Model of Solute Transport in a Single Fracture

3.2.1. ADE Model. The dispersive mass flux of the ADE model is proportional to the first-order spatial derivative of concentration. The one-dimensional governing equation of ADE is

$$\frac{\partial c}{\partial t} = D\frac{\partial^2 c}{\partial x^2} - v\frac{\partial c}{\partial x} \tag{7}$$

where c, D, and t denote the concentration of the solute, dispersion coefficient, and time, respectively.

3.2.2. TPL Model. The CTRW transport equation in Laplace is usually formulated to represent the time derivative in an algebraic expression. In one dimension, the Laplace transformed concentration $\tilde{c}$ (x,u) is given by

$$u\tilde{c}(x,u) - c_0(x) = -\tilde{M}(u)\left[v_\psi \frac{\partial}{\partial x}\tilde{c}(x,u) - D_\psi \frac{\partial^2}{\partial x^2}\tilde{c}(x,u)\right],$$
$$\tilde{M}(u) \equiv \bar{t}u\frac{\tilde{\psi}(u)}{1-\tilde{\psi}(u)}, \tag{8}$$

where u is the Laplace variable, the "~" symbol represents the Laplace transformed variable, $\bar{t}$ is a characteristic time, and v_ψ and D_ψ are the average transport velocity and generalized dispersion coefficient, respectively. The dispersivity can then be defined as $a_\psi = D_\psi/v_\psi$. It is important to note that the transport velocity can be different from the mean flow velocity. Also, the generalized dispersion coefficient is distinct from that in the ADE. It is noted also that the average mass flux of the solute, j, is defined in Laplace space through

$$\tilde{j} \equiv \tilde{M}v_\psi\left(\tilde{c} - \alpha_\psi\frac{\partial\tilde{c}}{\partial x}\right). \tag{9}$$

The function $\tilde{\psi}(u)$ is the heart of the CTRW formulation and characterizes the nature of the solute movement. The function $\tilde{M}(u)$ can take on several expressions, depending on the functional form of $\tilde{\psi}(u)$. General forms that have been described in the literature are

The truncated power-law model is

$$\tilde{\psi}(u) \equiv (1+\tau_2 u t_1)^\beta \exp(t_1 u)\frac{\Gamma\left(-\beta, \tau_2{}^{-1} + t_1 u\right)}{\Gamma\left(-\beta, \tau_2{}^{-1}\right)}, \quad 0 < \beta < 2, \tag{10}$$

where Γ is the incomplete Gamma function, t_1 is the lower limit time when the power-law behavior begins, and t_2 is the cut-off time describing the Fickian behavior. The parameter β indicates different types of anomalous transport.

4. Results and Discussion

4.1. Flow Characteristics. The Reynolds numbers calculated from (2) vary from 11.303 to 39.731 (see Table 1). For a single fracture with an aperture of 2 mm, the minimal Re value of 11.303 is obtained when v is 1.136×10^{-2} m/s and J is 0.050, while the maximal Re value of 39.731 is obtained when v is 3.993×10^{-2} m/s and J is 0.283. The range of Re is consistent with those of Iwai [33], Schrauf and Evans [34], and

Table 2: Fitted relation parameters of three formulas.

Darcy law		Forchheimer law			Izbash law		
K	R^2	a	b	R^2	n	λ	R^2
6.4114	0.9426	3.5204	89.086	0.9998	1.373	23.13	0.9996

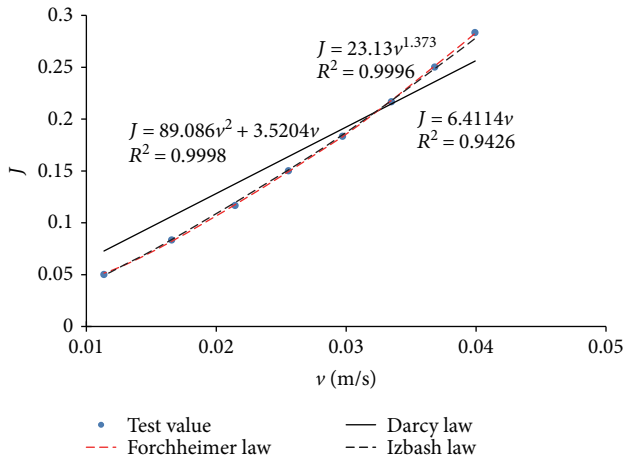

Figure 3: The relationship between the flow velocity and the hydraulic gradient.

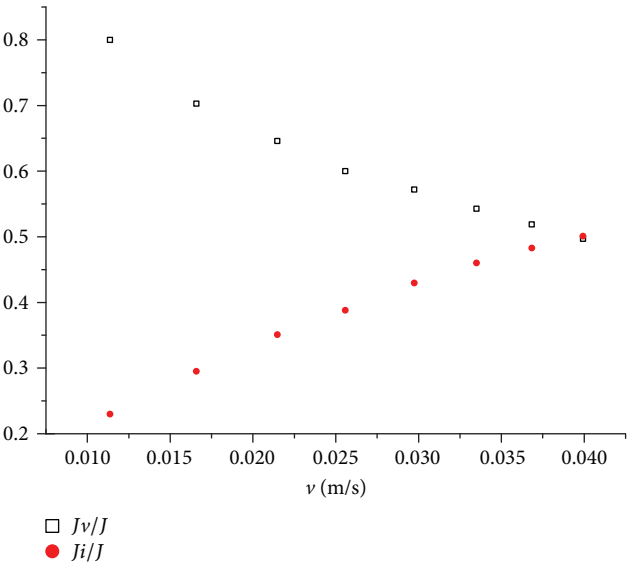

Figure 4: The relationship of Jv/J and Ji/J versus v.

Zimmerman and Yeo [35] who showed that turbulent flow can occur in a single fracture for Re greater than 10. A total of 8 groups of the flow velocity (v) and the hydraulic gradient (J) are obtained. The fitted results of Jv relationships are summarized in Table 2, and the fitted curves are shown in Figure 3.

From Table 2 and Figure 3, it is obvious that the relationship between the flow velocity and the hydraulic gradient (Jv) is not linear and it cannot be described by Darcy's law. The Jv relationship can be fitted by either the Forchheimer or the Izbash equation. The Forchheimer and Izbash equations can be expressed by $J = 89.086v^2 + 3.5204v$ and $J = 23.13v^{1.373}$, respectively. The correlation coefficients

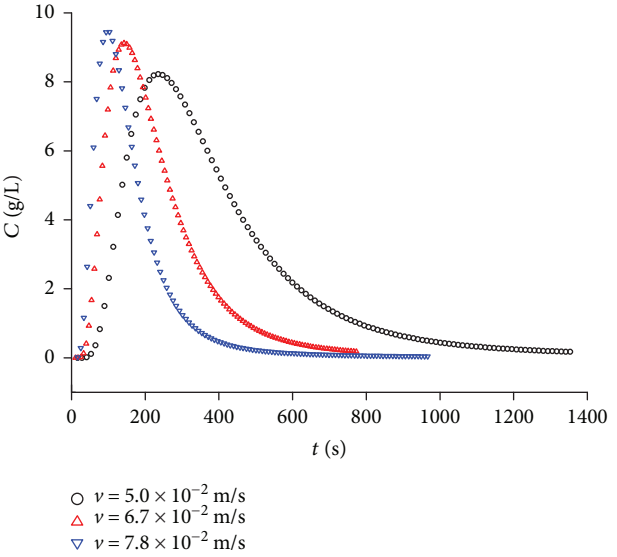

Figure 5: BTCs in fractures for the different velocities.

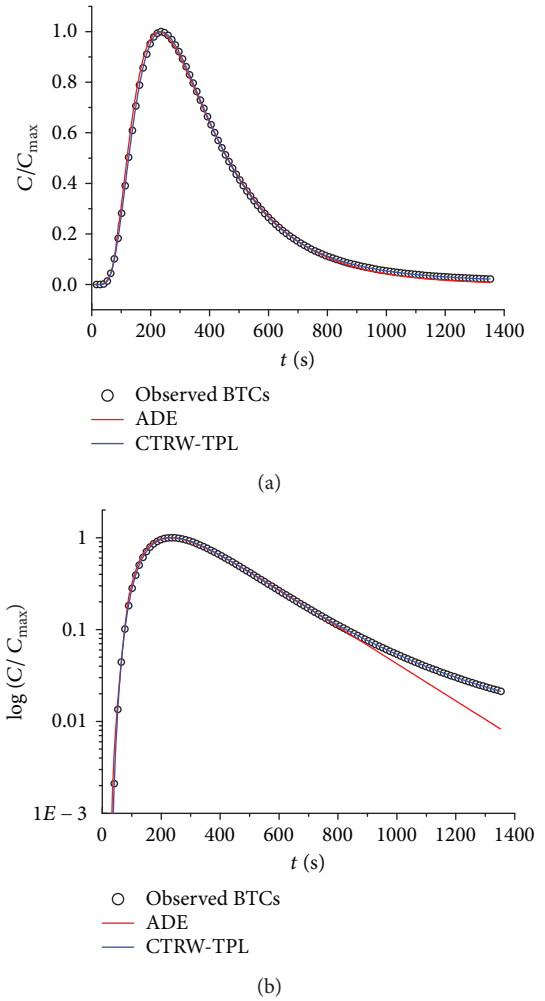

Figure 6: Comparison of fitted line of ADE and TPL when $v = 5.0 \times 10^{-2}$ m/s: (a) normal coordinate system; (b) semilog scale coordinate system.

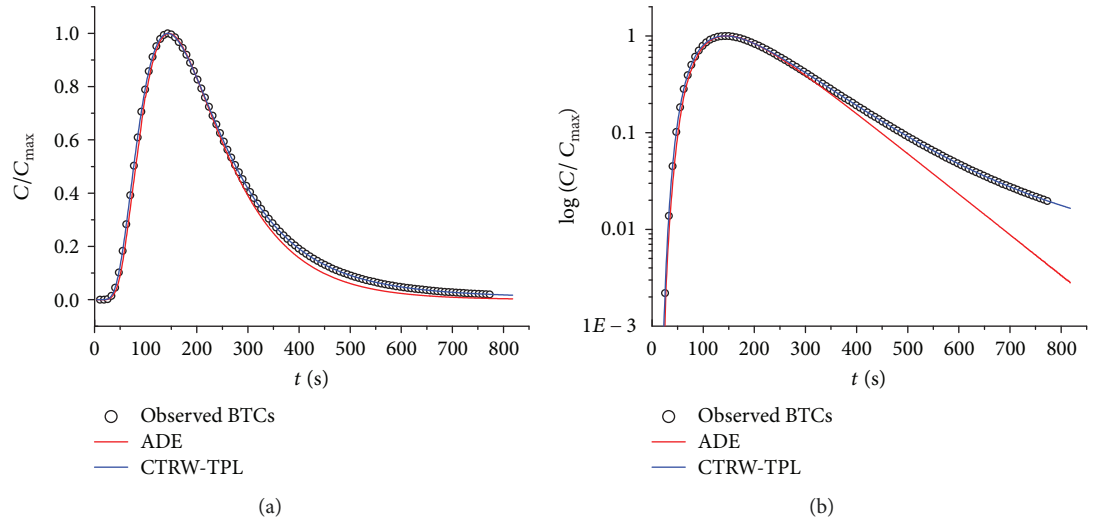

Figure 7: Comparison of ADE and TPL when $v = 6.7 \times 10^{-2}$ m/s: (a) normal coordinate system; (b) semilog scale coordinate system.

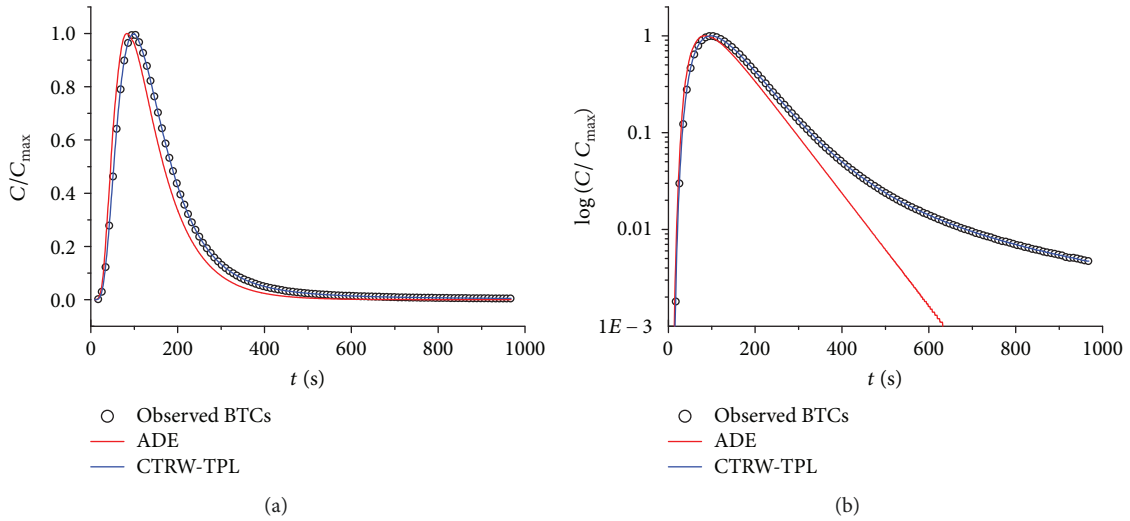

Figure 8: Comparison of ADE and TPL when $v = 7.8 \times 10^{-2}$ m/s: (a) normal coordinate system; (b) semilog scale coordinate system.

are 0.9998 and 0.9996, respectively. The Darcian equation can be expressed by $J = 6.4114v$; the correlation coefficient is 0.9426.

Comparison of Jv/J and Ji/J is shown in Table 1 and Figure 4. It can be seen that the value of Jv/J is decreasing and the value of Ji/J is increasing when $v > 10$ mm/s. In general, Jv/J and Ji/J have values within the same order of magnitude, meaning that both inertial and viscous flows are nonnegligible. So it is easily understandable to see that the existence of non-Darcian flow affects solute transport.

4.2. BTCs of Solute Transport. In the beginning, the tracer is injected by pulse mode from beginning to end. Concentration is monitored at the outlet end by electrical conductivity monitoring system. Figure 5 shows the BTCs of the tracer at three different velocities.

Figure 5 shows several important features of the tracer. Firstly, all the measured BTCs of the tracer exhibit the same trend, which is a non-Gaussian distribution with a long tailing. The long tailing demonstrates the non-Fickian transport in a single fracture of marble parallel plates. Secondly, with increasing flow velocity, the more the increase of the maximal value of concentration, the more the BTCs become narrow. Thirdly, the time of reaching peak value decreases with flow velocity decrease.

Table 3: The fitting parameters of BTCs at three velocities.

$V \times 10^{-2}$ m/s	ADE		TPL	
	r^2	RMSE	r^2	RMSE
5.0	0.9976	0.0157	0.9998	$1.26e-3$
6.7	0.9748	0.0507	0.9999	$1.20e-3$
7.8	0.9650	0.0521	0.9999	$1.32e-3$

4.3. Simulation Results of BTCs. In order to investigate the solute transport under the non-Darcian flow condition, both ADE and CTRW models are employed.

Table 4: The parameters of BTCs at three velocities.

V ($\times 10^{-2}$ m/s)	ADE		TPL				
	V_A ($\times 10^{-3}$ m/s)	D_A ($\times 10^{-4}$ m^2/s)	v_ψ ($\times 10^{-2}$ m/s)	D_ψ ($\times 10^{-4}$ m/s)	β	Lg (t_1)	Lg (t_2)
5.0	1.2	1.6	5.0	4.0	1.25	−1	6
6.7	2.4	2.2	7.2	6.0	1.3	−1.2	8
7.8	3.4	4.1	8.5	5.5	1.4	−0.5	10

Figures 6(a) and 6(b) show the observed and fitted BTCs when $v = 5.0 \times 10^{-2}$ m/s at a normal coordinate system and semilog scale coordinate system, Figures 7(a) and 7(b) show the observed and fitted BTCs when $v = 6.7 \times 10^{-2}$ m/s at a normal coordinate system and semilog scale coordinate system, and Figures 8(a) and 8(b) show the observed and fitted BTCs when $v = 7.8 \times 10^{-2}$ m/s at a normal coordinate system and semilog scale coordinate system. The estimated parameters of BTCs at three velocities are shown in Tables 3 and 4. As shown in Figures 6–8, the test data can be fitted by ADE and TPL models in a normal coordinate system. However, as shown in Figures 6(b)–8(b), the breakthrough curves fitted with ADE clearly indicate a deviating trend in a semilog scale coordinate system, especially for the tails of the breakthrough curves. Furthermore, with the increase of flow velocity, the breakthrough curves deviate more from the test values. It is found that TPL performs the best for fitting the test data than the ADE model in a normal coordinate system and in a semilog scale coordinate system.

Good performance of TPL as shown in Figures 6–8 is also reflected by the larger R^2 and smaller RMSE values than their counterparts resulting from the ADE model. The values of corresponding R^2 in the ADE model as shown in Table 3 are smaller than those of the TPL model. The values of RMSE in the ADE model as shown in Table 3 are larger than those of the TPL model.

From Table 4, one can see that the estimated values of dispersion coefficient (D) of ADE were smaller than those of TPL. In addition, the estimated β values in TPL were in the range of 1.25–1.4, which is less than 2, a value representing non-Fickian transport [36]. The values of the cut-off time (t_2) for the truncated power-law transition-time distribution function are larger than those of t_1 (a characteristic time). Therefore, the transition-time distribution is primarily controlled by β.

This study uses the CTRW calculation programs [29] and software of CXTFIT2.1 [35] to analyze BTCs in a single fracture of marble parallel plates and to evaluate its effect using r^2 and RMSE. These two indices are expressed by

$$r^2 = 1 - \frac{\sum_{i=1}^{N} (C_{io} - C_{ie})^2}{\sum_{i=1}^{N} (C_{io} - \bar{C}_{io})^2},$$
$$\text{RMSE} = \sqrt{\frac{1}{N} \sum_{i=1}^{N} (C_{io} - C_{ie})^2}, \quad (11)$$

where C_{io} and C_{ie} are observed and computed concentrations, respectively. N is number of measured values, and $\bar{C}_{io}$ is the mean of measured values. If the determination of r^2 is bigger and that of RMSE is smaller, the curve is better fitting.

5. Conclusion

This study aims to investigate the variations in flow velocity and solute transport in a fracture. A tracer experiment is carried out in a single fracture of marble parallel plate, in which sodium chloride (NaCl) is the tracer. Electrical conductivity was monitored during the sodium chloride solution injection period from the left fracture. Then the data were converted to concentrations according to the standard curve of NaCl, and the BTCs were fitted using ADE and CTRW.

From the analysis above, the following conclusions were drawn:

(1) The relationship between flow velocity (v) and hydraulic gradient (J) cannot be described by Darcy's law satisfactorily. Both Forchheimer and Izbash equations perform well in the Jv relationship.

(2) Breakthrough curves (BTCs) appear as obvious non-Fickian phenomena. With the increase of flow velocity, the peak value of concentration increases. With the increase of flow velocity, the time of reaching the peak value decreases.

(3) The ADE and TPL models have been used to fit the test values, while the results show that TPL model can best fit BTCs than the ADE model.

Conflicts of Interest

The authors declare that they have no conflicts of interest.

Acknowledgments

This research was partially supported by the National Natural Science Foundation of China (Grant nos. 41772250 and 41602256), the Science and Technology Fund of Land and Resources of Anhui Province (Grant no. 2016-k-11), and Shandong Province pilot program of science and technology on the construction of water eco-civilization. The authors sincerely thank Dr. Quanrong Wang (China University of Geosciences) for his editing on the final version of this manuscript. The authors also thank Dr. Fulin Li (Shandong Institute of Water Science and Technology, Jinan) for his funding help in the experiment.

References

[1] Y. Huang, Z. F. Zhou, L. Li, and J. Chen, "Experimental investigation of solute transport in unsaturated fractured rock," *Environmental Earth Sciences*, vol. 73, no. 12, pp. 8379–8386, 2015.

[2] S. A. Junejo, Q. Y. Zhou, M. A. Talpur, D. Wang, and J. L. Yang, "Quantification of electrical resistance to estimate NaCl behavior in a column under controlled conditions," *Geochemistry International*, vol. 52, no. 9, pp. 794–804, 2014.

[3] A. Kemna, J. Vanderborght, B. Kulessa, and H. Vereecken, "Imaging and characterisation of subsurface solute transport using electrical resistivity tomography (ERT) and equivalent transport models," *Journal of Hydrology*, vol. 267, no. 3-4, pp. 125–146, 2002.

[4] P. D. Jackson, K. J. Northmore, P. I. Meldrum et al., "Non-invasive moisture monitoring within an earth embankment—a precursor to failure," *NDT & E International*, vol. 35, no. 2, pp. 107–115, 2002.

[5] J. Z. Qian, H. B. Zhan, Z. Chen, and H. Ye, "Experimental study of solute transport under non-Darcian flow in a single fracture," *Journal of Hydrology*, vol. 399, no. 3-4, pp. 246–254, 2011.

[6] A. Nowammooz, G. Radilla, M. Fourar, and B. Berkowitz, "Non-Fickian transport in transparent replicas of rough-walled rock fractures," *Transport in Porous Media*, vol. 98, no. 3, pp. 651–682, 2013.

[7] Y. F. Tan, *Research on Flow and Solute Transport in a Single Fracture, [Ph.D. thesis]*, Hohai University, Nanjing, China, 2010.

[8] J. G. Wang and Z. F. Zou, "Testing study on solute transport in fracture media," *Chinese Journal of Rock Mechanics and Engineering*, vol. 24, no. 5, pp. 829–834, 2005.

[9] Y. F. Tan and Z. F. Zhou, "Understanding and treatment of digital images of dye tracers in solute transport experiments," *Hydrogeology & Engineering*, vol. 112, no. 1, pp. 99–101, 2007.

[10] J. G. Wang and Z. F. Zhou, "Testing study on solute transport in fracture media," *Chinese Journal of Rock Mechanics and Engineering*, vol. 24, no. 5, pp. 829–834, 2005.

[11] J. Z. Qian, H. B. Zhan, W. D. Zhao, and F. G. Sun, "Experimental study of turbulent unconfined groundwater flow in a single fracture," *Journal of Hydrology*, vol. 311, no. 1-4, pp. 134–142, 2005.

[12] J. Z. Qian, Z. Chen, H. B. Zhan, and H. C. Guan, "Experimental study of the effect of roughness and Reynolds number on fluid flow in rough-walled single fractures: a check of local cubic law," *Hydrological Processes*, vol. 25, no. 4, pp. 614–622, 2011.

[13] J. Z. Qian, Z. Chen, H. B. Zhan, and S. H. Luo, "Solute transport in a filled single fracture under non-Darcian flow," *International Journal of Rock Mechanics and Mining Sciences*, vol. 48, no. 1, pp. 132–140, 2011.

[14] Z. Wen, G. H. Huang, and H. B. Zhan, "Non-Darcian flow in a single confined vertical fracture toward a well," *Journal of Hydrology*, vol. 330, no. 3-4, pp. 698–708, 2006.

[15] Q. R. Wang, H. B. Zhan, and Y. X. Wang, "Non-Darcian effect on slug test in a leaky confined aquifer," *Journal of Hydrology*, vol. 527, pp. 747–753, 2015.

[16] M. Javadi, M. Sharifzadeh, and K. Shahriar, "A new geometrical model for non-linear fluid flow through rough fractures," *Journal of Hydrology*, vol. 389, no. 1-2, pp. 18–30, 2010.

[17] C. Cherubini, C. I. Giasi, and N. Pastore, "Evidence of non-Darcy flow and non-Fickian transport in fractured media at laboratory scale," *Hydrology and Earth System Sciences*, vol. 17, no. 7, pp. 2599–2611, 2013.

[18] F. Bauget and M. Fourar, "Non-Fickian dispersion in a single fracture," *Journal of Contaminant Hydrology*, vol. 100, no. 3-4, pp. 137–148, 2008.

[19] J. Hadermann and W. Heer, "The Grimsel (Switzerland) migration experiment: integrating field experiments, laboratory investigations and modelling," *Journal of Contaminant Hydrology*, vol. 21, no. 1–4, pp. 87–100, 1996.

[20] L. D. McKay, W. E. Sanford, and J. M. Strong, "Field-scale migration of colloidal tracers in a fractured shale saprolite," *Groundwater*, vol. 38, no. 1, pp. 139–147, 2000.

[21] G. Kosakowski, B. Berkowitz, and H. Scher, "Analysis of field observations of tracer transport in a fractured till," *Journal of Contaminant Hydrology*, vol. 47, no. 1, pp. 29–51, 2001.

[22] I. Neretnieks, T. Eriksen, and P. Tahtinen, "Tracer movement in a single fissure in granitic rock: some experimental results and their interpretation," *Water Resources Research*, vol. 18, no. 4, pp. 849–858, 1982.

[23] M. W. Becker and A. M. Shapiro, "Tracer transport in fractured crystalline rock: evidence of nondiffusive breakthrough tailing," *Water Resources Research*, vol. 36, no. 7, pp. 1677–1686, 2000.

[24] F. J. Jimenez-Hormero, J. V. Giraldez, A. Laguna, and Y. Pachepsky, "Continuous time random walks for analyzing the transport of a passive tracer in a single fissure," *Water Resources Research*, vol. 41, no. 4, article W04009, 2005.

[25] M. Fourar, "Characterization of heterogeneities at the core-scale using the equivalent stratified porous medium approach," in *Proceedings of the International Symposium of the Society of Core Analysts*, pp. 1–6, Trondheim, Norway, September 2006.

[26] B. Berkowitz, A. Cortis, M. Dentz, and H. Scher, "Modeling non-Fickian transport in geological formations as a continuous time random walk," *Reviews of Geophysics*, vol. 44, no. 2, article RG2003, 2006.

[27] M. Levy and B. Berkowitz, "Measurement and analysis of non-Fickian dispersion in heterogeneous porous media," *Journal of Contaminant Hydrology*, vol. 64, no. 3-4, pp. 203–226, 2003.

[28] Y. W. Xiong, G. H. Huang, and G. Z. Huang, "Modeling solute transport in one-dimensional homogeneous and heterogeneous soil columns with continuous time random walk," *Journal of Contaminant Hydrology*, vol. 86, no. 3-4, pp. 163–175, 2006.

[29] B. Berkowitz and H. Scher, "Exploring the nature of non-Fickian transport in laboratory experiments," *Advances in Water Resources*, vol. 32, no. 5, pp. 750–755, 2009.

[30] G. Y. Gao, H. B. Zhan, S. Y. Feng, G. Huang, and X. Mao, "Comparison of alternative models for simulating anomalous solute transport in a large heterogeneous soil column," *Journal of Hydrology*, vol. 377, no. 3-4, pp. 391–404, 2009.

[31] B. Berkowitz, G. Kosakowski, G. Margolin, and H. Scher, "Application of continuous time random walk theory to tracer test measurements in fractured and heterogeneous porous media," *Groundwater*, vol. 39, no. 4, pp. 593–604, 2001.

[32] X. S. Yan, J. Z. Qian, B. Y. Chen, L. Ma, and X. P. Zhou, "Experimental and simulated study of water flow and transport in a single fracture of marble parallel plates," *Chinese Journal of Hydrodynamics*, vol. 29, no. 5, pp. 524–528, 2014.

[33] K. Iwai, *Fundamental Studies of the Fluid Flow through a Single Fracture, [Ph.D. thesis]*, University of California, Berkeley, California, 1976.

[34] T. W. Schrauf and D. D. Evans, "Laboratory studies of gas flow through a single natural fracture," *Water Resources Research*, vol. 22, no. 7, pp. 1038–1050, 1986.

[35] R. W. Zimmerman and I. W. Yeo, "Fluid flow in rock fractures: from the Navier-Stokes equations to the cubic law," *Dynamics of Fluids in Fractured Rock*, vol. 122, pp. 213–224, 2000.

[36] Y. W. Xiong, G. H. Huang, and Q. Z. Huang, "Model solute transport in heterogeneous soil column using continuous time random walk," *Advances in Water Science*, vol. 17, no. 6, 2006.